PHYS 122 / FINAL PROJECT

Quasilinear Transport in Tokamak Core

From slab drift-wave response
to gyrokinetic transport and its validation

Zhifei Gui

Department of Physics and Astronomy, Dartmouth College

November 12 2026

Outline

1 Slab drift waves: response to flux

2 From slab response to gyrokinetic closure

3 Numerical tests of the response

4 From response tests to prediction

5 Conclusions

1. Start with a slab drift-wave model

Geometry and equilibrium

$$\mathbf{B} = B\hat{\mathbf{z}}, \quad x: \text{ radial}, \quad z: \text{ parallel}.$$

Collisionless, electrostatic electrons; constant T_e and a slowly varying density $n_0(x)$.

$$F_0 = n_0(x)\left(\frac{m_e}{2\pi T_e}\right)^{3/2} e^{-m_e v^2/(2T_e)}.$$

Perturbation and gradient drive

$$\widetilde{\phi} = \mathrm{Re}\left[\hat{\phi} e^{i(k_y y + k_\parallel z - \omega t)}\right].$$

$$L_n^{-1} = -\frac{d\ln n_0}{dx}, \qquad \omega_* = \frac{k_y T_e}{eBL_n} = k_y v_{de}.$$

Take $e > 0$, $q_e = -e$ and $k_\perp \rho_e \ll 1$. The density gradient is the free-energy source.

Electron drift-kinetic equation

$$\partial_t f_e + \mathbf{v}_E \cdot \nabla_\perp f_e + v_\parallel \partial_z f_e - \frac{e}{m_e} E_\parallel \partial_{v_\parallel} f_e = 0, \qquad \mathbf{v}_E = \frac{\mathbf{E}\times\mathbf{B}}{B^2}. \tag{1}$$

2. Linearize to obtain the electron response

Write $f_e = F_0 + \widetilde{f}_e$ and retain first-order terms:

$$-i(\omega - k_\parallel v_\parallel)\hat{f}_{e1} + \frac{\hat{E}_y}{B}\partial_x F_0 - \frac{e}{m_e}\hat{E}_\parallel \partial_{v_\parallel} F_0 = 0. \tag{2}$$

$$\partial_x F_0 = -\frac{F_0}{L_n}, \quad \partial_{v_\parallel} F_0 = -\frac{m_e v_\parallel}{T_e} F_0, \quad \hat{E}_y = -ik_y\hat{\phi}, \quad \hat{E}_\parallel = -ik_\parallel\hat{\phi}.$$

Substitute and solve for $\hat{f}_{e1}$

$$\boxed{\hat{f}_{e1} = \frac{e\hat{\phi}F_0}{T_e}\frac{\omega_* - k_\parallel v_\parallel}{\omega - k_\parallel v_\parallel} = \frac{e\hat{\phi}F_0}{T_e}\left[1 - \frac{\omega - \omega_*}{\omega - k_\parallel v_\parallel}\right].} \tag{3}$$

Adiabatic part: in phase with ϕ; Kinetic/Diabatic part: contains the resonance $\omega \simeq k_\parallel v_\parallel$.

Drift-kinetic derivation, following Goldston (1995), Ch. 26.

3. Velocity integration produces a phase-shifted density

$$\hat{n}_e = \int d^3v\, \hat{f}_{e1} = \frac{n_0 e\hat{\phi}}{T_e}\left[1 - (\omega - \omega_*)\mathcal{I}(\omega)\right], \tag{4}$$

$$\mathcal{I}(\omega) = \frac{1}{n_0}\int d^3v\, \frac{F_0}{\omega - k_\parallel v_\parallel}.$$

The causal (Landau) prescription determines how the resonance pole is passed. For $|\omega_r| \ll |k_\parallel| v_{te}$ and weak growth,

$$\mathcal{I} \simeq -i\sqrt{\frac{\pi}{2}}\frac{1}{|k_\parallel| v_{te}}, \qquad v_{te} = \sqrt{T_e/m_e}.$$

The imaginary response is the phase information

$$\boxed{\frac{\hat{n}_e}{\hat{\phi}} \simeq \frac{n_0 e}{T_e}(1 - i\delta)}, \qquad \delta = \sqrt{\frac{\pi}{2}}\frac{\omega_* - \omega_r}{|k_\parallel| v_{te}}. \tag{5}$$

4. Average particle conservation to identify the flux

Integrating the drift-kinetic equation over velocity gives

$$\partial_t n_e + \nabla_\perp \cdot (n_e \mathbf{v}_E) + \partial_z (n_e u_\parallel) = 0. \tag{6}$$

Average over periodic y and z

$$n_e = n_0(x,t) + \widetilde{n}_e, \quad v_{E,x} = \widetilde{v}_x,$$

$$\langle \widetilde{n}_e \rangle = \langle \widetilde{v}_x \rangle = 0.$$

Parallel and y-derivative terms average to zero; radial divergence remains.

Slow profile evolution

$$\boxed{\partial_t n_0 + \partial_x \Gamma = 0}, \tag{7}$$

$$\boxed{\Gamma \equiv \langle \widetilde{n}_e \widetilde{v}_x \rangle}. \tag{8}$$

Each fluctuation is first order, but their correlation is second order. Quasilinear theory evaluates this correlation using the linear response.

5. The phase-shifted response produces radial transport

For real fields, $\langle AB \rangle = \frac{1}{2}\,\mathrm{Re}(\hat{A}\hat{B}^*)$, and $\hat{v}_x = -ik_y\hat{\phi}/B$. Therefore,

$$\Gamma_k = \frac{1}{2}\,\mathrm{Re}(\hat{n}_e\hat{v}_x^*) = -\frac{k_y}{2B}|\hat{\phi}|^2\,\mathrm{Im}\left(\frac{\hat{n}_e}{\hat{\phi}}\right) = \boxed{\frac{n_0 e k_y}{2BT_e}|\hat{\phi}|^2\delta}. \tag{9}$$

Physical picture: choose $\phi = \Phi\cos\theta$

$$\widetilde{v}_x = \frac{k_y\Phi}{B}\sin\theta,$$

$$\widetilde{n}_e = \frac{n_0 e\Phi}{T_e}(\cos\theta + \delta\sin\theta).$$

The $\cos\theta\sin\theta$ term averages to zero. The $\delta\sin^2\theta$ term survives.

The general response–intensity form

$$\frac{\hat{n}_e}{\hat{\phi}} = A_k e^{-i\alpha_k}, \qquad \Gamma_k = \underbrace{\frac{k_y}{2B}A_k\sin\alpha_k}_{W_k^\Gamma}|\hat{\phi}|^2. \tag{10}$$

Both phase and amplitude ratio determine the response weight W_k^Γ

Gyrokinetics keeps the response–flux structure

A schematic local, collisionless electrostatic response is

$$g_{s,k} \sim J_0 \frac{q_s \phi_k}{T_s} F_{0s} \frac{\omega - \omega_{*s}^{v}}{\omega - k_{\parallel} v_{\parallel} - \omega_{Ds}}. \tag{11}$$

What the slab illustration leaves out

- Finite Larmor radius: J_0 gyroaveraging.
- Magnetic curvature and gradient drifts: ω_{Ds}.
- Toroidal geometry, trapped particles and temperature-gradient drives.

What carries over

1. Solve linear response and quasineutrality.
2. Take density or energy moments.
3. Correlate with radial $E \times B$ motion.

$$F_a^{\mathrm{QL}} = \sum_k W_{a,k}^{\mathrm{linear}} I_k^{\mathrm{sat}}.$$

Antonsen & Lane (1980); Staebler et al. (2024), Sec. 2.

The approximation has two ingredients

$$F_a^{\mathrm{QL}} = \sum_k \underbrace{W_{a,k}^{\mathrm{linear}}}_{\text{response weight}} \underbrace{I_k^{\mathrm{sat}}}_{\text{potential intensity}}, \qquad F_a \in \{\Gamma, Q_i, Q_e\}.$$

What linear theory supplies

The complex moment-to-potential ratio:

$$\frac{\delta n_k}{\delta \phi_k} = \left|\frac{\delta n_k}{\delta \phi_k}\right| e^{-i\alpha_k}.$$

Both **cross-phase** and **amplitude ratio** enter the weight.

What requires nonlinear information

$$I_k = \langle |\delta \phi_k|^2 \rangle_t.$$

An eigenmode has arbitrary overall amplitude. Prediction needs a **saturation rule**.

Nonlinear saturation supplies the missing amplitude

Turbulence saturates before profiles relax in Tokamak

$$t_{\mathrm{NL}} \sim \frac{a}{c_s}, \quad t_{\mathrm{profile}} \sim \frac{a}{c_s}\rho_*^{-2}. \tag{12}$$

For $\rho_* \equiv \rho_s/a \ll 1$, nonlinear mode coupling acts while equilibrium gradients are nearly fixed.

Small fluctuations $\neq$ negligible nonlinear saturation.

In classical QLT

$$\tau_w \ll t_{\mathrm{eq}} \ll t_{\mathrm{nl}} \tag{13}$$

- $\tau_w \ll t_{\mathrm{eq}}$: First average the phases, then evolve the background.
- $t_{\mathrm{eq}} \ll t_{\mathrm{nl}}$: Saturation must be achieved by the quasi-linear mechanism itself.

What must be tested in the gyrokinetic closure?

The practical problem

Core profiles evolve slowly, but their turbulent fluxes depend on fast microscopic fluctuations.

- Nonlinear gyrokinetics resolves the turbulence.
- Reduced quasilinear models supply fluxes for repeated profile calculations.

Three questions for the evidence

1. Does the **linear response** give the right correlations?
2. Does response plus **saturation** predict nonlinear fluxes?
3. Do predicted **fluctuations and profiles** agree with experiment?

Validation sequence: response weights $\rightarrow$ complete fluxes $\rightarrow$ experimental phases and profiles.

Framework: Staebler et al., Nuclear Fusion 64, 103001 (2024).

A controlled test supplies the nonlinear intensity

Waltz et al. (2009): local GYRO

- Electrostatic, collisionless, ion-scale turbulence.
- ITG/TEM and TEM cases with kinetic electrons.
- ITG-ae: ion-temperature-gradient turbulence with adiabatic electrons.

Hold the intensity fixed

$$F^{\mathrm{QL}} = \sum_k W_k^{\mathrm{QL}} I_k^{\mathrm{NL}}. \tag{14}$$

Compare with F^{NL} from the same turbulent state.

$$O_\alpha \equiv \frac{F_\alpha^{\mathrm{QL}}}{F_\alpha^{\mathrm{NL}}} \qquad (\text{“overage”}). \tag{15}$$

A discrepancy diagnoses the **response approximation**. No fitted saturation rule is being tested here.

mQLTA and fQLTA ask different response questions

m: mode-based test

$$F_m^{\mathrm{QL}} = \sum_k W_{k,\mathrm{lead}} I_k^{\mathrm{NL}}. \tag{16}$$

One leading eigenmode at each k receives the full nonlinear intensity.

Input: a linear eigenmode and the nonlinear k spectrum.
Question: is that mode representative of the turbulent mixture?

f: frequency-based test

$$F_f^{\mathrm{QL}} = \sum_k \int \frac{d\omega}{2\pi} W_k(\omega) S_k^{\mathrm{NL}}(\omega). \tag{17}$$

A linear tracer responds to the full time-dependent nonlinear potential.

Input: the complete frequency spectrum.

The plasma stays nonlinear. Only the response used to calculate the test flux changes.

Heat-channel errors are largely a common offset

Reported mQLTA overages

Case	O_{Q_i}	O_{Q_e}
ITG/TEM	1.47	1.70
TEM1	1.45	1.37
TEM2	1.69	1.85

Across all nine published channel/case entries: mean 1.64, normalized scatter 13.5% rms.

ITG/TEM: changing the response test

Channel	mQLTA	fQLTA
Ion energy	1.47	1.48
Electron energy	1.70	1.15

The electron channel changes substantially; the ion channel barely changes.

A common factor can be calibrated: $C \simeq 1/1.64$. The useful evidence is the relative consistency of channels, not exact equality to nonlinear fluxes.

Errors at weakly populated scales matter less

Electron-energy overage

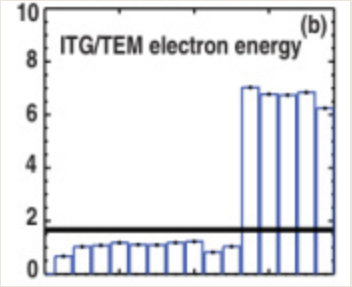

x-axis:$k_y\rho_s$.
Overage(per $k_y\rho_s$ bin):

$$O_{\alpha,k} \equiv \frac{W^{\mathrm{QL}}_{\alpha,k} I_k}{F^{\mathrm{NL}}_{\alpha,k}}$$

Nonlinear potential intensity

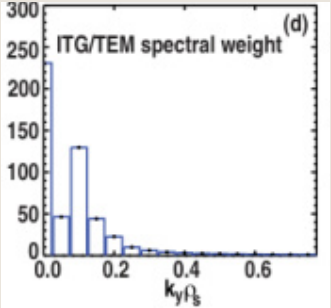

Nonlinear spectral weight I_k (per $k_y\rho_s$ bin).

A gradient scan separates heat from particle transport

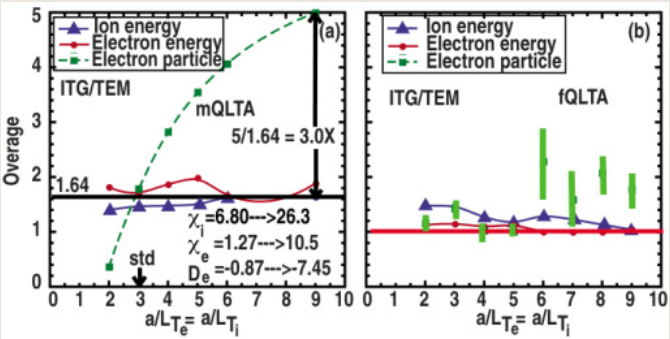

Heat: approximately stable overages

Energy transport grows by roughly 4–8×, while response-test ratios change relatively little.

Particles: increasing mismatch

Strongly inward particle flux separates from the heat channels, in both mQLTA and fQLTA.

The phase comparison locates a particle-channel error

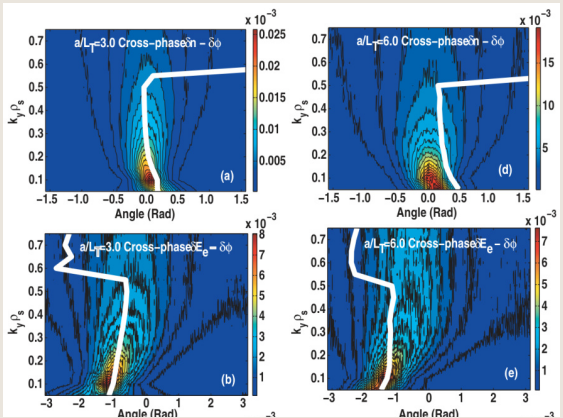

- White line: Cross-phase of linear eigenmodes $\vartheta_k^{\mathrm{lin}}$.
- Contours: Nonlinear cross-phase $\vartheta_k^{\mathrm{NL}}$

- Left/right: $a/L_T = 3$ and 6.
- Top: density–potential phase.
- Bottom: electron energy–potential phase.

The actual cross-phase for Γ is small, whereas the linear model yields an overestimated cross-phase at $a/L_T = 6$, indicating a significant phase deviation.

A correct phase is not sufficient: ITG(adiabatic electrons)

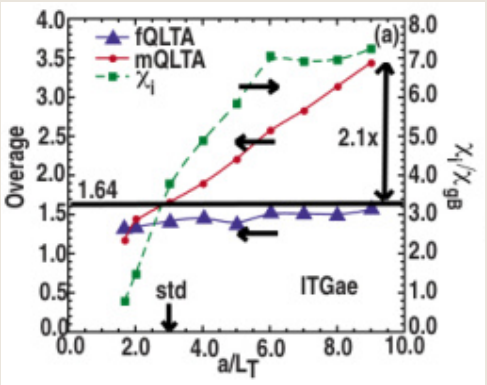

- With adiabatic electrons, the mQLTA ion-energy overage grows.
- The fQLTA overage stays nearly flat.
- The reported pressure–potential phase still tracks the nonlinear phase.

fQLTA is more accurate(?). This is because fQLTA convolves the full nonlinear frequency spectrum. In contrast, mQLTA assigns the entire intensity at each wavenumber to a single, most unstable eigenmode.

The complete model must also predict the intensity

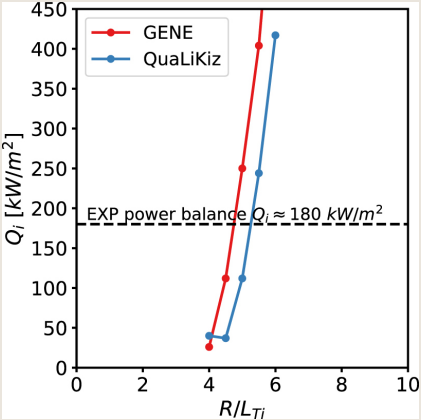

Ion heat flux in ion temperature gradient scans.

QuaLiKiz versus nonlinear GENE

JET hybrid 94875, $\rho = 0.65$; collisionless comparison in $\hat{s}$–α geometry.

- The tested flux contains **both** response and saturation prescription.
- At power-balance flux, required R/L_{T_i} agrees within 10%.
- Similar slope tests stiffness: $\partial Q_i / \partial (R/L_{T_i})$.

Transport simulations are flux-driven: the heating power that we know determines the flux, and the gradients are what get solved for. Therefore, the meaningful approach is to compare gradients at a fixed flux.

Getting profiles from local fluxes

$$\frac{3}{2}\frac{\partial(n_s T_s)}{\partial t} + \frac{1}{V'}\frac{\partial}{\partial r}\left[V'(Q_s^{\mathrm{QL}} + Q_s^{\mathrm{neo}})\right] = S_{E,s}, \quad V' = \frac{\mathrm{d}V}{\mathrm{d}r}. \tag{18}$$

$$\frac{\partial n_s}{\partial t} + \frac{1}{V'}\frac{\partial}{\partial r}\left[V'\left(\Gamma_s^{\mathrm{QL}} + \Gamma_s^{\mathrm{neo}}\right)\right] = S_s, \qquad V' = \frac{dV}{dr}. \tag{19}$$

One transport-solver step

1. Profiles determine local gradients.
2. QL response + saturation give local fluxes.
3. Particle and energy balances update profiles.

Application: JET core profiles

JETTO supplies transport evolution; QuaLiKiz supplies the turbulent closure. Sources, neoclassical transport, initial conditions and the boundary at $\rho = 0.85$ are additional inputs.

The application: profiles with prescribed boundaries

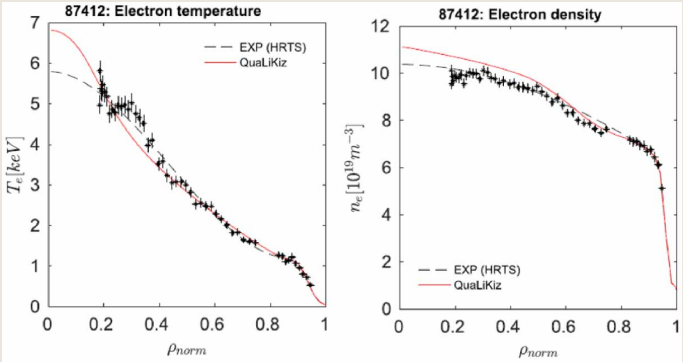

JET baseline 87412

JETTO + QuaLiKiz predicts T_e and n_e and compares them with HRTS measurements.

In the gradient region (approximately $0.3 < \rho < 0.85$), the predictions and measurements agree within the range of data scatter.

Conclusions: What makes the QL closure useful?

1. **A robust structure:** gradients create kinetic responses; phase-shifted correlations carry particle and energy fluxes.

2. **Qualified numerical support:** dominant heat-transport scales often retain useful linear responses; strong particle pinches and amplitude-ratio errors expose limits.

3. **A separate saturation problem:** response tests, complete-flux benchmarks and experimental validation establish different parts of the model.

Key Points

Nonlinear turbulence can retain approximately linear transport correlations. Combined with a validated saturation model, this enables practical core-profile prediction.

Appendix: what selects the slab drift-wave frequency?

Close the electron response with cold-ion continuity and momentum, including ion polarization:

$$\frac{\hat{n}_i}{n_0 e\hat{\phi}/T_e} = \frac{\omega_*}{\omega} + \frac{k_\parallel^2 c_s^2}{\omega^2} - k_y^2\rho_s^2, \qquad c_s^2 = \frac{T_e}{m_i}, \quad \rho_s = \frac{c_s}{\Omega_i}.$$

Quasineutrality: $\hat{n}_i = \hat{n}_e$

$$1 - i\delta = \frac{\omega_*}{\omega} + \frac{k_\parallel^2 c_s^2}{\omega^2} - k_y^2\rho_s^2.$$

In the drift-wave limit $|k_\parallel| c_s \ll |\omega_r| \ll |k_\parallel| v_{te}$, neglect parallel ion motion. For $|\delta| \ll 1$,

$$\omega_r \simeq \frac{\omega_*}{1 + k_y^2\rho_s^2}, \qquad \gamma \simeq \frac{\omega_r \delta}{1 + k_y^2\rho_s^2}.$$

For $k_y > 0$ and $dn_0/dx < 0$: $\omega_r < \omega_*$ gives $\delta > 0$, growth and outward particle flux.

Report's cold-ion closure, following Goldston (1995), Ch. 26; local $k_x = 0$ slab example.

Appendix: simulation scope and interpretation

GA standard ITG/TEM case

$$q = 2, \quad \hat{s} = 1, \quad R/a = 3, \quad r/a = 0.5,$$

$$T_i/T_e = 1, \qquad \sqrt{m_i/m_e} = 60,$$

$$a/L_{T_i} = a/L_{T_e} = 3, \qquad a/L_n = 1.$$

Circular $\hat{s}$–α geometry, $\alpha = 0$; electrostatic, collisionless; no equilibrium rotation shear.

How to interpret the ratios

- A common O can be absorbed by one intensity calibration.
- A changing O across channels or gradients cannot be fixed by one factor.
- Near $\Gamma = 0$, use absolute flux errors or the zero-flux gradient, not $\Gamma_{\mathrm{QL}}/\Gamma_{\mathrm{NL}}$.

Waltz et al. (2009), Sec. III. These tests do not establish validity for arbitrary ITER parameters or electromagnetic regimes.

Appendix: mode and frequency response kernels

In Waltz's convention, $R_{s,k} = \delta n_{s,k}/\delta\phi_k$, $W_{s,k} = (ck_y/B)\,\mathrm{Im}\,R_{s,k}$, and $\varpi_s^v = k_\parallel v_\parallel + \omega_{Ds}$.

Mode: evaluate at a complex eigenfrequency

$$W_{s,km} = \frac{ck_y}{B}\frac{q_s n_0}{T_s}\int d^3v\, F_0 J_0^2(\omega_{*s}^v - \varpi_s^v)\frac{\gamma_k^m}{(\varpi_s^v - \omega_k^m)^2 + (\gamma_k^m)^2}.$$

Frequency: causal response on the real axis

$$W_{s,k}(\omega) = \pi\frac{ck_y}{B}\frac{q_s n_0}{T_s}\int d^3v\, F_0 J_0^2(\omega_{*s}^v - \varpi_s^v)\delta(\omega - \varpi_s^v).$$

Integrating the second kernel against $S_k(\omega)$ includes the entire prescribed frequency spectrum, rather than assigning it to the leading eigenmode.

Waltz et al. (2009); report appendix. Gaussian units; q_s is signed and F_0 is unit normalized.

Appendix: why tracer ambipolarity is different

Self-consistent electrostatic modes

$$\sum_s q_s \delta n_s = 0 \quad \Rightarrow \quad \sum_s q_s \Gamma_s = 0.$$

Quasineutrality constrains species responses to a shared potential.

Passive linear tracers

Each species responds to the imposed nonlinear potential. Its density does not enter the field solve.

$$\sum_s q_s \delta n_s^{\mathrm{tracer}} = 0$$

is therefore not imposed.

Tracer charge-flux imbalance is not a charge-conservation failure of the plasma. The discussed fQLTA particle comparison uses the electron tracer flux.

Waltz et al. (2009), discussion of fQLTA and tracer transport.

References I

1. G. Staebler, C. Bourdelle, J. Citrin and R. Waltz, “Quasilinear theory and modelling of gyrokinetic turbulent transport in tokamaks,” *Nuclear Fusion* **64**, 103001 (2024). doi:10.1088/1741-4326/ad6ba5

2. R. E. Waltz, A. Casati and G. M. Staebler, “Gyrokinetic simulation tests of quasilinear and tracer transport,” *Physics of Plasmas* **16**, 072303 (2009). doi:10.1063/1.3167391

3. R. J. Goldston, *Introduction to Plasma Physics* (1995), Ch. 26, drift-kinetic equation and kinetic drift waves.

4. T. M. Antonsen and B. Lane, *Physics of Fluids* **23**, 1205–1214 (1980). doi:10.1063/1.863121

References II

5. J. Citrin et al., “Integrated modelling and multiscale gyrokinetic validation study of ETG turbulence in a JET hybrid H-mode scenario,” *Nuclear Fusion* **62**, 086025 (2022). doi:10.1088/1741-4326/ac7535

6. A. E. White et al., “Measurements of the cross-phase angle between density and electron temperature fluctuations and comparison with gyrokinetic simulations,” *Physics of Plasmas* **17**, 056103 (2010). doi:10.1063/1.3323084

7. J. Citrin et al., “Tractable flux-driven temperature, density, and rotation profile evolution with the quasilinear gyrokinetic transport model QuaLiKiz,” *Plasma Physics and Controlled Fusion* **59**, 124005 (2017). doi:10.1088/1361-6587/aa8aeb